

2018-07

Damage mapping after the 2017 Puebla Earthquake in Mexico using high-resolution Alos2 Palsar2 data

Bruno Adriano, Shunichi Koshimura, Sadra Karimzadeh, Masashi Matsuoka, Magaly Koch.
2018. "Damage Mapping After the 2017 Puebla Earthquake in Mexico Using High-Resolution Alos2 Palsar2 Data." IGARSS 2018 - 2018 IEEE International Geoscience and Remote Sensing Symposium. IGARSS 2018 - 2018 IEEE International Geoscience and Remote Sensing Symposium. 2018-07-22 - 2018-07-27. <https://doi.org/10.1109/igarss.2018.8517933>
<https://hdl.handle.net/2144/40349>

"Downloaded from OpenBU. Boston University's institutional repository."

DAMAGE MAPPING AFTER THE 2017 PUEBLA EARTHQUAKE IN MEXICO USING HIGH-RESOLUTION ALOS2 PALSAR2 DATA

Bruno Adriano^{1*}, *Shunichi Koshimura*², *Sadra Karimzadeh*³, *Masashi Matsuoka*³, and *Magaly Koch*⁴

¹Geoinformatics Unit, RIKEN Center for Advanced Intelligence Project, Japan

²International Research Institute of Disaster Science, Tohoku University, Japan

³Department of Architecture and Building Engineering, Tokyo Institute of Technology, Japan

⁴Center for Remote Sensing, Boston, USA

ABSTRACT

On September 19, 2017, the Mw7.1 Puebla Earthquake caused significant destruction in several cities in central Mexico. In this paper, two pre- and one post-event ALOS2-PALSAR2 data were used to detect the damaged area around Izucar de Matamoros town in Mexico. First, we identify the built-up areas using pre-event data. Second, we evaluate the earthquake-induced damage areas using an RGB color-coded image constructed from the pre- and co-event coherence images. Our analysis showed that the green and red bands display a great potential to discriminate the damaged areas.

1. INTRODUCTION

Space-borne Earth observation is a suitable alternative for grasping the damage situation after the occurrence of a disaster. In this context, synthetic aperture radar (SAR) sensors have an important advantage over optical sensor due to their capability of observing the Earth's surface in all weather and daylight conditions. The new generation of high-resolution SAR platforms, such as the ALOS2-PALSAR2 and TerraSAR-X, provide valuable information that can be used to detect and extract damaged areas after disasters [1, 2, 3, 4].

Generally, there are two main approaches for damage assessment using SAR data. The first one is based on a change detection analysis using a set of pre- and post-event

SAR images. This approach explores the relationship between the damaged areas and the difference- and correlation-coefficients calculated from the dataset [5, 6, 7]. The second approach is based on the application of machine learning algorithms that classify the damaged areas using a set of images features such as color and texture [4, 3, 8, 9]. However, both approaches mainly utilize the intensity information of the SAR images. Here, we introduce a preliminary method using the phase information to extract damage areas from SAR images. This methodology is applied to detect the damaged areas following the 2017 Mw7.1 Mexico earthquake.

2. STUDY AREA AND SAR DATA

This study focuses on the Izucar de Matamoros town that is located approximately 20 km northeast of the epicenter (Fig. 1). This city was one of the hardest hit places by the earthquake. According to the local newspaper, on September 20 (one day after the main-shock) there were 43 people killed, and over 3,000 buildings were severely damaged or destroyed.

The SAR dataset is composed of three ALOS2-PALSAR2 SAR images, two pre-event scenes acquired on January 25, 2017 (T1) and September 6, 2017 (T0); the latest was captured almost two weeks before the main-shock. The post-event scene was acquired on September 20, 2017 (T2), one day after the earthquake. The incident angle at the center of the images was 36.2° . All PALSAR2 data were captured with dual-polarization (HH-HV) in ascending path (STRIPMAP SM3 mode) and were provided as Single-look-

* This research was supported by the Japan Society for the Promotion of Science (JSPS-Grants: P16055, 17H06108, and P16380) and the JST/JICA, SATREPS (Science and Technology Research Partnership for Sustainable Development) Project.

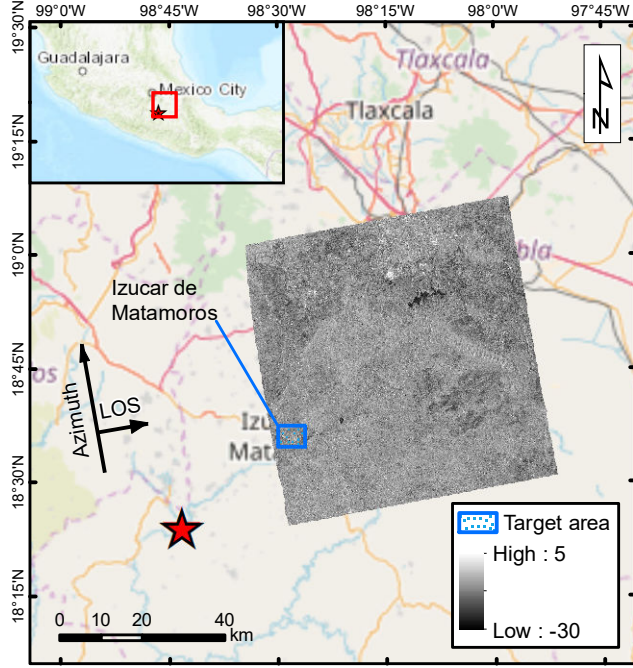


Fig. 1. View of the study area and the ALOS2-PALSAR2 images used in this study. The location map is shown on the top-left corner. The red star shows the location of the epicenter of the 2017 Puebla Earthquake. The blue rectangle shows the location of the study area. The intensity image shows the PALSAR2 data coverage. The black arrows indicate the azimuth and range directions of the PALSAR data.

complex and Slant-range (SCSB) data in processing level 1.1. Multi-Look processing was applied to reduce the speckle noise; then the images were geocoded and calibrated using the ENVI/SARscape software version 5.2. The 30 m Shuttle Radar Topography Mission (SRTM) dataset (Ver. 3) was employed for the geocoding and orthorectification. The enhanced Lee filter [10] was applied to the sigma naught PALSAR2 intensity images to reduce speckle effect. For minimizing the loss of information, the window size of the filter was set as 5×5 pixels [11]. Finally, all PALSAR2 images were resampled at 10 m/pixel in a square size. Also, a GIS vector data of building footprints of Izucar de Matamoros town, which includes a post-event damage assessment (Fig. 2b), downloaded from the United Nations Institute for Training and Research (UNITAR) website was used as a reference to verify the accuracy of our damage mapping.

3. METHODOLOGY

First, we calculate the built-up area using the speckle-divergency coefficient calculated from the pre-event SAR data (T0) [12, 3, 11]. The SAR interferogram coherence evaluates the correlation of the phase information between two SAR images [13]. Our methodology detects the damaged areas by constructing a coherence-based RGB-composited image [14].

Second, we calculate a pre-event coherence image (γ_a) using the January 25 (slave image) and September 9 dataset (master image). The co-event coherence (γ_b) is calculated from the September 9 SAR data (master image) and the September 20 image (slave image). The pre- and the co-event coherence values were calculated in the slant range images from the complex data. The primary assumption is that after the earthquake the collapsed building and debris changed the ground surface. Thus, the co-event coherence decreased drastically compared with the pre-event coherence. To enhance the coherence characteristics, we construct an RGB color-coded image as shown in Eq. 1-3. Finally, the RGB color-coded image is masked using the estimated built-up area.

$$R = \gamma_a - \gamma_b \quad (1)$$

$$G = \gamma_a + \gamma_b \quad (2)$$

$$B = \frac{\gamma_a + \gamma_b}{2} \quad (3)$$

4. RESULTS AND DISCUSSION

The comparison between the preliminary mapping result and the ground truth data (GTD) of building damage, downloaded from UNITAR website, is shown in Fig. 2. Panel (a) shows the result of the RGB color-coded image constructed from the pre- and co-event coherence. The green color indicates the vegetation areas within the built-up region (magenta). The red spots indicate areas where the co-event coherence decreased after the earthquake. These spots, therefore, may indicate areas where collapsed buildings or debris occur. The mean value of the red, green, and blue channels are -0.45, 0.45, and 0.39, respectively. The visual comparison of both panels shows that the proposed methodology shows good agreement

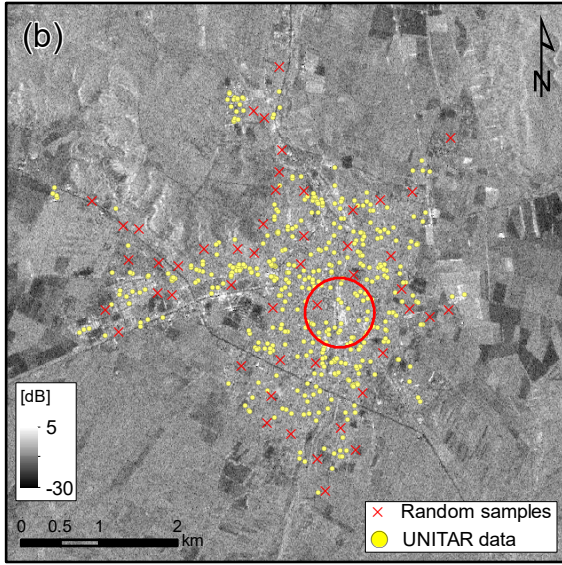
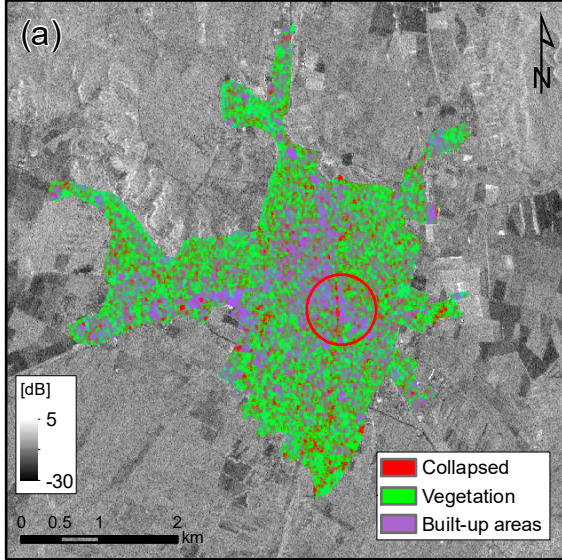


Fig. 2. Damage mapping at the Izucar de Matamoros town. (a) The color-coded image constructed by using the pre- and co-event coherence images. The background image corresponds to the post-event PALSARs image. (b) Ground truth data of building damage downloaded from UNITAR website.

with the UNITAR’s GTD. The method shows good correlation with the number of collapsed buildings around the center of the Izucar de Matamoros town (red circle in Fig. 2). Furthermore, some buildings along the boundary of the built-up area are also well estimated.

To validate our method, we randomly selected 50 points from the GTD and the non-damaged built-up areas (red cross in Fig. 2b). Then, we calculate the box plot graph from the

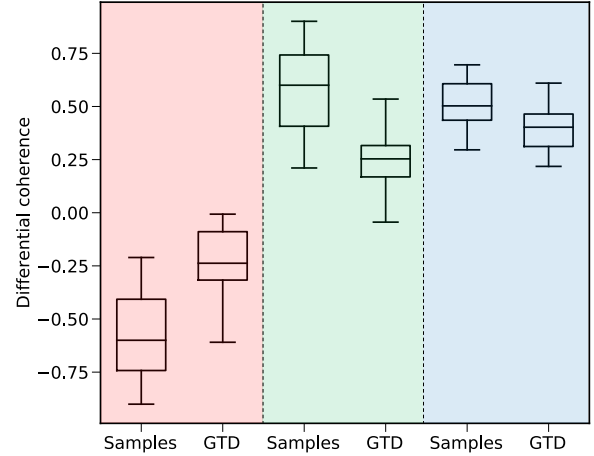


Fig. 3. Box plots of the 50 points randomly selected in the GTD and non-damaged built-up areas from each band of the RGB color-coded image.

pixel values of each band of the RGB color-coded image, as shown in Fig. 3. The red and green bands show significant performance to discriminate both groups (damage areas according to the GTD and the no-damage built-up areas). For instance, in case of the green band, over 78% of the points from the damaged areas are greater than the non-damage samples from the built-area. On the other hand, the red band shows that about 75% of the GTD samples are less than non-damage samples. The blue band, however, shows less potential to differentiate both classes where about only 25% of the samples from the GTD are less than the non-damage samples from the built-up areas.

5. CONCLUSION

The proposed method shows great potential for detecting damaged areas. Further analysis can be applied for semi-automatic classification and extraction of collapsed buildings. Therefore, the temporal coherence-based analysis provides reliable information to be used in emergency response after natural disasters provided that the resolution of images is enough to represent building footprint areas.

6. REFERENCES

- [1] Adamo Ferro, Dominik Brunner, and Lorenzo Bruzzone, “Automatic Detection and Reconstruction of

- Building Radar Footprints From Single VHR SAR Images,” *IEEE Transactions on Geoscience and Remote Sensing*, vol. 51, no. 2, pp. 935–952, feb 2013.
- [2] Bruno Adriano, Erick Mas, Shunichi Koshimura, Hideomi Gokon, Wen Liu, and Masashi Matsuoka, “Developing a method for urban damage mapping using radar signatures of building footprint in SAR imagery: A case study after the 2013 Super Typhoon Haiyan,” in *2015 IEEE International Geoscience and Remote Sensing Symposium (IGARSS)*. jul 2015, pp. 3579–3582, IEEE.
- [3] Yanbing. Bai, Bruno. Adriano, Erick. Mas, and Shunichi. Koshimura, “Machine learning based building damage mapping from the ALOS-2/PALSAR-2 SAR imagery: Case study of 2016 kumamoto earthquake,” *Journal of Disaster Research*, vol. 12, no. Special Issue, 2017.
- [4] Yanbing Bai, Chang Gao, Sameer Singh, Magaly Koch, Bruno Adriano, Erick Mas, and Shunichi Koshimura, “A Framework of Rapid Regional Tsunami Damage Recognition From Post-event TerraSAR-X Imagery Using Deep Neural Networks,” *IEEE Geoscience and Remote Sensing Letters*, vol. 1, pp. 1–5, 2017.
- [5] Hiroyuki Miura, Saburoh Midorikawa, and Masashi Matsuoka, “Building Damage Assessment Using High-Resolution Satellite SAR Images of the 2010 Haiti Earthquake,” *Earthquake Spectra*, vol. 32, no. 1, pp. 591–610, feb 2016.
- [6] Wen Liu, Fumio Yamazaki, Hideomi Gokon, and Shunichi Koshimura, “Extraction of Tsunami-Flooded Areas and Damaged Buildings in the 2011 Tohoku-Oki Earthquake from TerraSAR-X Intensity Images,” *Earthquake Spectra*, vol. 29, no. S1, pp. S183–S200, mar 2013.
- [7] Hideomi Gokon, Shunichi Koshimura, and Masashi Matsuoka, “Object-Based Method for Estimating Tsunami-Induced Damage Using TerraSAR-X Data,” *Journal of Disaster Research*, vol. 1, no. 2, pp. 225–235, 2016.
- [8] Marc Wieland, Wen Liu, and Fumio Yamazaki, “Learning Change from Synthetic Aperture Radar Images: Performance Evaluation of a Support Vector Machine to Detect Earthquake and Tsunami-Induced Changes,” *Remote Sensing*, vol. 8, no. 10, pp. 792, 2016.
- [9] Luis Moya, Luis Marval Perez, Erick Mas, Bruno Adriano, Shunichi Koshimura, and Fumio Yamazaki, “Novel Unsupervised Classification of Collapsed Buildings Using Satellite Imagery, Hazard Scenarios and Fragility Functions,” *Remote Sensing*, vol. 10, no. 2, pp. 296, feb 2018.
- [10] Armand Lopes, Ridha Touzi, and E. Nezry, “Adaptive speckle filters and scene heterogeneity,” *IEEE Transactions on Geoscience and Remote Sensing*, vol. 28, no. 6, pp. 992–1000, 1990.
- [11] Yanbing Bai, Bruno Adriano, Erick Mas, Hideomi Gokon, and Shunichi Koshimura, “Object-Based Building Damage Assessment Methodology Using Only Post Event ALOS-2/PALSAR-2 Dual Polarimetric SAR Intensity Images,” *Journal of Disaster Research*, vol. 12, no. 2, pp. 259–271, mar 2017.
- [12] Thomas Esch, Andreas Schenk, Tobias Ullmann, Michael Thiel, Achim Roth, and Stefan Dech, “Characterization of Land Cover Types in TerraSAR-X Images by Combined Analysis of Speckle Statistics and Intensity Information,” *IEEE Transactions on Geoscience and Remote Sensing*, vol. 49, no. 6, pp. 1911–1925, jun 2011.
- [13] Sadra Karimzadeh and Masashi Matsuoka, “Building damage assessment using multisensor dual-polarized synthetic aperture radar data for the 2016 M 6.2 Amatrice earthquake, Italy,” *Remote Sensing*, vol. 9, no. 4, 2017.
- [14] Sadra Karimzadeh and Masashi Matsuoka, “Building Damage Characterization for the 2016 Amatrice Earthquake Using Ascending- Descending COSMO-SkyMed Data and Topographic Position Index,” *IEEE Journal of Selected Topics in Applied Earth Observations and Remote Sensing*, 2018.